4-1-2018

Development of a pulmonary imaging biomarker pipeline for phenotyping of chronic lung disease

Fumin Guo

Dante Capaldi

Miranda Kirby

Khadija Sheikh

Sarah Svenningsen

See next page for additional authors

Citation of this paper:
Guo, F., Capaldi, D., Kirby, M., Sheikh, K., Svenningsen, S., McCormack, D. G., Fenster, A., Parraga, G., & Canadian Respiratory Research Network (2018). Development of a pulmonary imaging biomarker pipeline for phenotyping of chronic lung disease. Journal of medical imaging (Bellingham, Wash.), 5(2), 026002. https://doi.org/10.1117/1.JMI.5.2.026002

Journal of Medical Imaging

MedicalImaging.SPIEDigitalLibrary.org

Development of a pulmonary imaging biomarker pipeline for phenotyping of chronic lung disease

Fumin Guo
Dante Capaldi
Miranda Kirby
Khadija Sheikh
Sarah Svenningsen
David G. McCormack
Aaron Fenster
Grace Parraga

SPIE.

Fumin Guo, Dante Capaldi, Miranda Kirby, Khadija Sheikh, Sarah Svenningsen, David G. McCormack, Aaron Fenster, Grace Parraga, , "Development of a pulmonary imaging biomarker pipeline for phenotyping of chronic lung disease," *J. Med. Imag.* **5**(2), 026002 (2018), doi: 10.1117/1.JMI.5.2.026002.

Development of a pulmonary imaging biomarker pipeline for phenotyping of chronic lung disease

Fumin Guo,[a,b,c] Dante Capaldi,[a,d] Miranda Kirby,[e] Khadija Sheikh,[a] Sarah Svenningsen,[a] David G. McCormack,[f] Aaron Fenster,[a,b,d] Grace Parraga,[a,b,d,*] and for the Canadian Respiratory Research Network
[a]University of Western Ontario, Robarts Research Institute, London, Ontario, Canada
[b]University of Western Ontario, Graduate Program in Biomedical Engineering, London, Ontario, Canada
[c]University of Toronto, Sunnybrook Research Institute, Toronto, Canada
[d]University of Western Ontario, Department of Medical Biophysics, London, Ontario, Canada
[e]University of British Columbia, St. Paul's Hospital, Centre for Heart Lung Innovation, Vancouver, Canada
[f]University of Western Ontario, Division of Respirology, Department of Medicine, London, Ontario, Canada

Abstract. We designed and generated pulmonary imaging biomarker pipelines to facilitate high-throughput research and point-of-care use in patients with chronic lung disease. Image processing modules and algorithm pipelines were embedded within a graphical user interface (based on the .NET framework) for pulmonary magnetic resonance imaging (MRI) and x-ray computed-tomography (CT) datasets. The software pipelines were generated using C++ and included: (1) inhaled $^{3}He/^{129}Xe$ MRI ventilation and apparent diffusion coefficients, 2)) CT-MRI coregistration for lobar and segmental ventilation and perfusion measurements, (3) ultrashort echo-time ^{1}H MRI proton density measurements, (4) free-breathing Fourier-decomposition ^{1}H MRI ventilation/perfusion and free-breathing ^{1}H MRI specific ventilation, (5) multivolume CT and MRI parametric response maps, and (6) MRI and CT texture analysis and radiomics. The image analysis framework was implemented on a desktop workstation/tablet to generate biomarkers of regional lung structure and function related to ventilation, perfusion, lung tissue texture, and integrity as well as multiparametric measures of gas trapping and airspace enlargement. All biomarkers were generated within 10 min with measurement reproducibility consistent with clinical and research requirements. The resultant pulmonary imaging biomarker pipeline provides real-time and automated lung imaging measurements for point-of-care and high-throughput research. [DOI: 10.1117/1.JMI.5.2.026002]

Keywords: magnetic resonance imaging; thoracic computed tomography; image processing, biomarkers; asthma; chronic obstructive lung disease.

Paper 17360RR received Dec. 12, 2017; accepted for publication Jun. 14, 2018; published online Jun. 28, 2018.

1 Introduction

For chronic lung diseases such as asthma and chronic obstructive lung disease (COPD), x-ray computed tomography (CT) is considered the gold standard imaging method.[1] Quantitative lung CT analyses have been used in large-scale studies, such as NETT,[2] SARP,[3] MESA-lung,[4] COPDGene,[5] CanCOLD,[6] ECLIPSE,[7] and SPIROMICS,[8] and these have enabled a deeper understanding of lung disease pathophysiology. CT provides unique imaging biomarkers of airway and parenchymal abnormalities,[9] including lung volumes and density, parenchyma morphology, airway dimensions, and regional air trapping. Notably, CT image analysis tools have been developed and validated for pulmonary biomarkers, including pulmonary Workstation^{R} and Apollo^{R} (VIDA Diagnostic Inc., Corallville, Iowa), thoracic VCAR (General Electric Healthcare, Milwaukee), Pulmo3D (Fraunhofer MEVIS, Bremen, Germany), pulmonary module (Mimics Innovation Suite, Materialise, Leuven, Belgium), chest imaging platform (Brigham and Women's Hospital, Boston, Massachusetts), FLUIDDA (FLUIDDA nv, Kontich, Belgium), and pulmonary toolkit (available in a Github repository: https://github.com/tomdoel/pulmonarytoolkit). Pulmonary studies[3,5–7,10,11] have used these tools, some of which have gained regulatory approval (e.g., Apollo^{R} and thoracic VCAR) for research and clinical use.

Magnetic resonance imaging (MRI) also provides lung functional and microstructural biomarkers but it is much less commonly used. In particular, inhaled hyperpolarized noble gas ($^{3}He/^{129}Xe$) MRI visualizes inhaled gas distribution[12] and provides measurements of parenchyma integrity.[13,14] ^{1}H-MRI using both conventional[15] and oxygen-enhanced approaches[16] also reveals lung structural and functional abnormalities[17] and response to treatment.[18] In a similar manner, ultrashort echo-time (UTE) MRI provides improved visualization of lung anatomy and microstructure,[19,20] while Fourier decomposition (FD) may be used to generate pulmonary ventilation and perfusion maps.[21,22] A number of studies have demonstrated the potential for pulmonary MRI biomarkers, including longitudinal[23–25] and observational[26,27] investigations and treatment response or image-guided evaluations.[28–32]

Until now, lung MRI has not been used in multicenter research studies or trials and clinical use remains very minimal. This is primarily due to challenges,[33,34] including the lack of user-friendly, point-of-care image processing tools to rapidly generate quantitative lung MRI measurements.[33,34] Therefore, our objective was to embed lung MRI and CT biomarker

*Address all correspondence to: Grace Parraga, E-mail: gparraga@robarts.ca

2329-4302/2018/$25.00 © 2018 SPIE

pipelines within a user-friendly graphical user interface (GUI) that integrated software modules for validated and emerging biomarkers of lung structure and function.

2 Materials and Methods

2.1 *Overview of Algorithms and Pipelines*

We developed a pulmonary imaging biomarker framework using Microsoft Visual Studio 2013 (Microsoft Corporation, Redmond, Washington) based on the .NET framework (Microsoft Corporation, Redmond, Washington) using the following software development process: (1) requirement identification, (2) design, (3) implementation, and (4) verification and maintenance. First, we identified application-specific requirements with local collaborating clinicians who specifically asked for this tool for use in clinic. Software design was proposed based on the application requirements, timelines, familiarity with development tools, functionality provided by existing tools, and agreement on coding style. The entire design step was divided into multiple short stages reviewed by the developer team and clinicians/end users, and each stage was broken down into multiple subtasks that were entered into a task tracker. Each developer worked on a subtask and submitted code to a shared version control system. In addition, automated test modules were written for each subtask and shared within the developer team. Changes to previous implementations were reviewed by other members and integrated into the main branch upon agreement. Documentation was also created for the project and updated at each step and stage. Products from each stage were demonstrated to the developer team and clinicians/end users, and feedback was collected and integrated into the next stage. After software prototype release, users reported issues or desired features to the developer team through issue tracker and/or via email. The developer team assessed the issues and requirements, added new tasks when necessary, and released updated versions of the code/executables to users.

As shown in Fig. 1, this tool incorporates multiview three-dimensional (3-D) volume rendering,[35] surface rendering [using Visualization Toolkit (VTK)[36]], image seeding, blending/overlapping, zooming in/out, fiducial placement, and dimension measurements. The resulting tool provides biomarkers derived from hyperpolarized $^{3}He/^{129}Xe$ static ventilation, diffusion weighted MRI, anatomical ^{1}H, UTE, two-dimensional (2-D)/3-D free-breathing MRI as well as integration and coregistration of MRI with CT volumes. After scanning, the scanner automatically stores image data on the picture archiving and communication system (PACS) server in DICOM format. A PACS client (i.e., K-PACS) is installed on a desktop workstation or tablet that is directly connected to ethernet or via USB-to-ethernet adapters (not wireless transmissions). The PACS server and client identify each other by their network addresses, communication ports, and application entry titles. The PACS client queries and retrieves DICOM data from the server to the local hard drive following DICOM protocols. The downloaded images are entered into the software framework, and biomarker quantification workflow starts on the desktop workstation or tablet. DICOM images and analyze, nifty formats are commonly provided by other systems and are supported by our software framework using VTK[36] and GDCM (DICOM toolkit).[37] All user interface functionality is provided by the .NET framework and the 3-D visualization system, which was developed in our lab for 3-D ultrasound imaging.[38,39] No other libraries are used in our application. As shown in schematic in Fig. 2, image processing and analysis modules were integrated within the GUI that were previously developed and validated across a wide range of pulmonary abnormalities[19,21,40–44] by our group using C++/CUDA (CUDA v6.0, NVIDIA Crop., Santa Clara, California) and implemented for Windows operating systems (Microsoft Corporation, Redmond, Washington). The derived imaging measurements are displayed with the GUI, presented to end users, saved to hard drive (DICOM images and/or numerical values in spreadsheet files), and sent back to the PACS server for archiving.

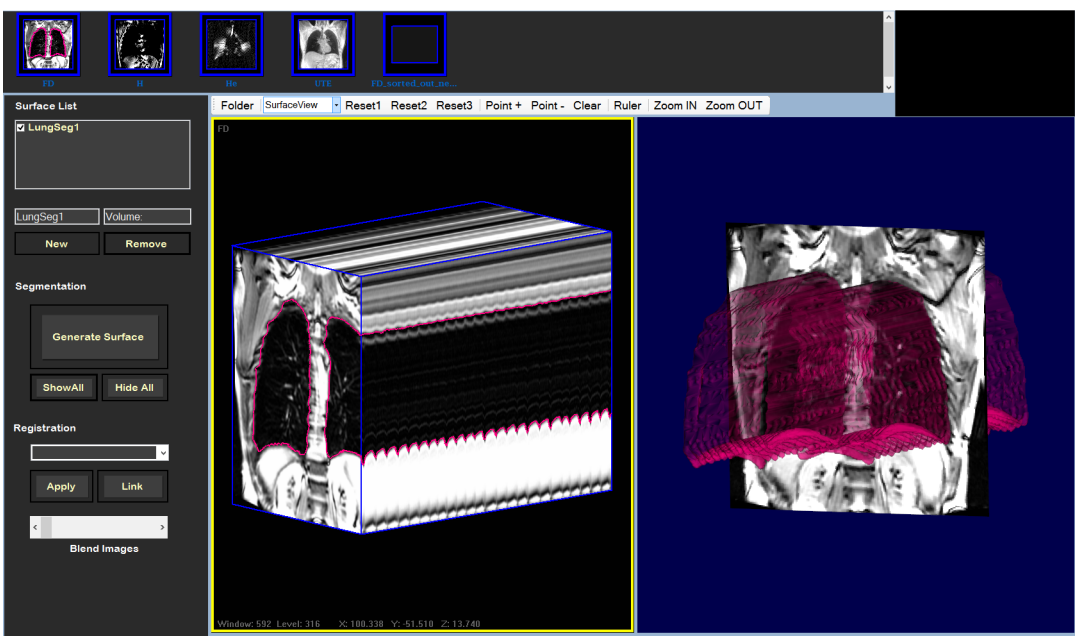

Fig. 1 Pulmonary imaging biomarker graphical user interface.

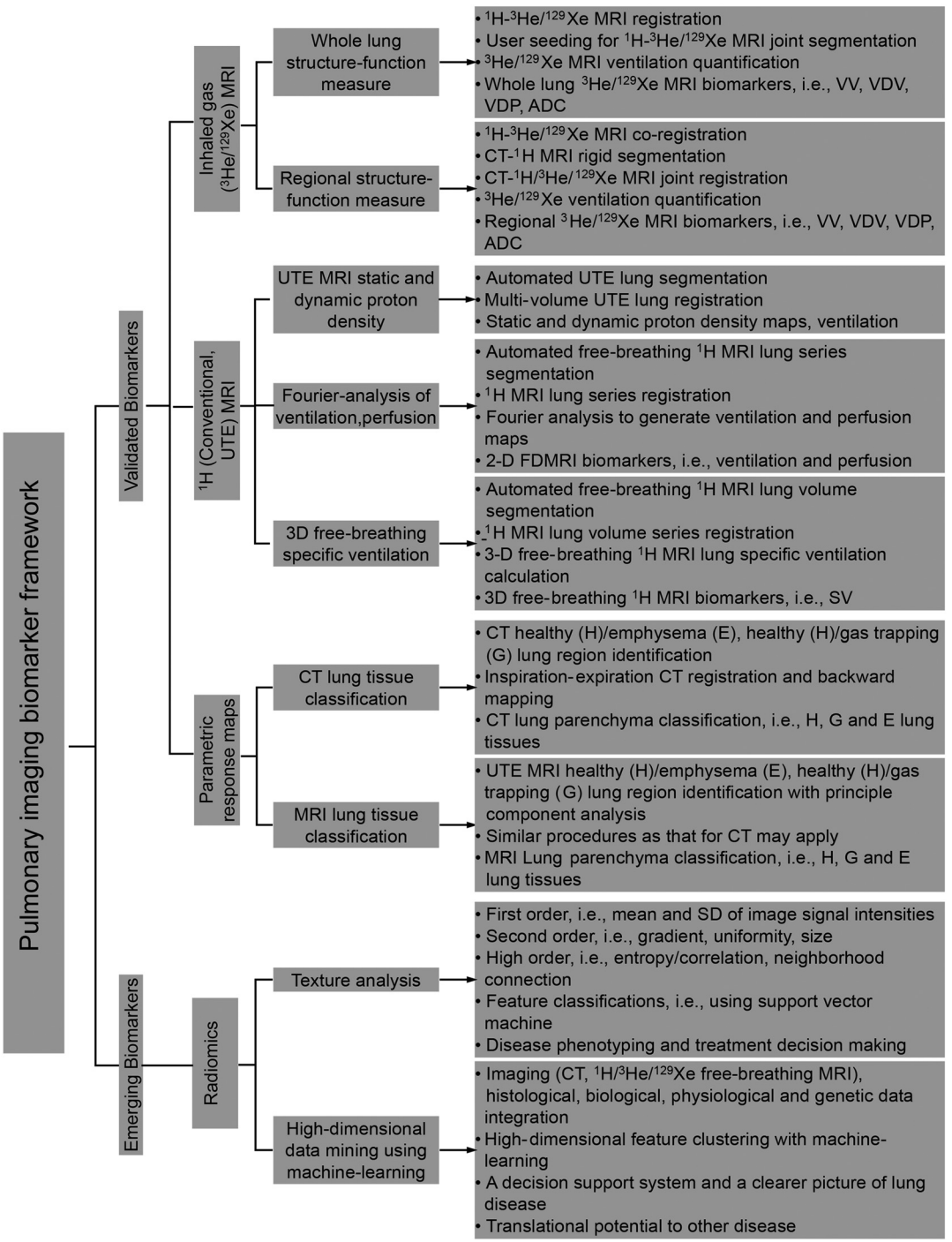

Fig. 2 Schematic for image processing and analysis modules provided by the pulmonary imaging biomarker approach.

As shown in Fig. 3, this approach currently includes: (A) whole lung and regional inhaled ^{3}He/^{129}Xe MRI structure–function, (B) UTE MRI static and dynamic proton density, (C) FD free-breathing ^{1}H MRI ventilation/perfusion, (D) free-breathing ^{1}H MRI specific ventilation (SV), and (E) CT and MRI parametric response maps (RPMs), and radiomic biomarkers (not shown here). In particular, the CT airway tree in (A) and segmented inspiration/expiration CT lung in (E) are reproductions provided by Pulmonary Workstation 2.0 (VIDA Diagnostic Inc., Corallville, Iowa). The linear regression in (B) and sinusoidal curves and the SV calculation equation in (D) are illustrations of the respective biomarker workflow. All the other elements including lung CT/MRI registration, segmentation contours, structure–function maps, and numerical values of relevant biomarkers are provided by the software. We note that these intermediate and final outputs may be helpful to: (1) better understand the processing steps of each biomarker module, (2) validate the calculation of biomarkers by referring back to the information the calculations are based on, (3) provide more insights into the spatial–temporal abnormalities of pulmonary disease, and (4) discover and report issues or bugs of software by developers and end users.

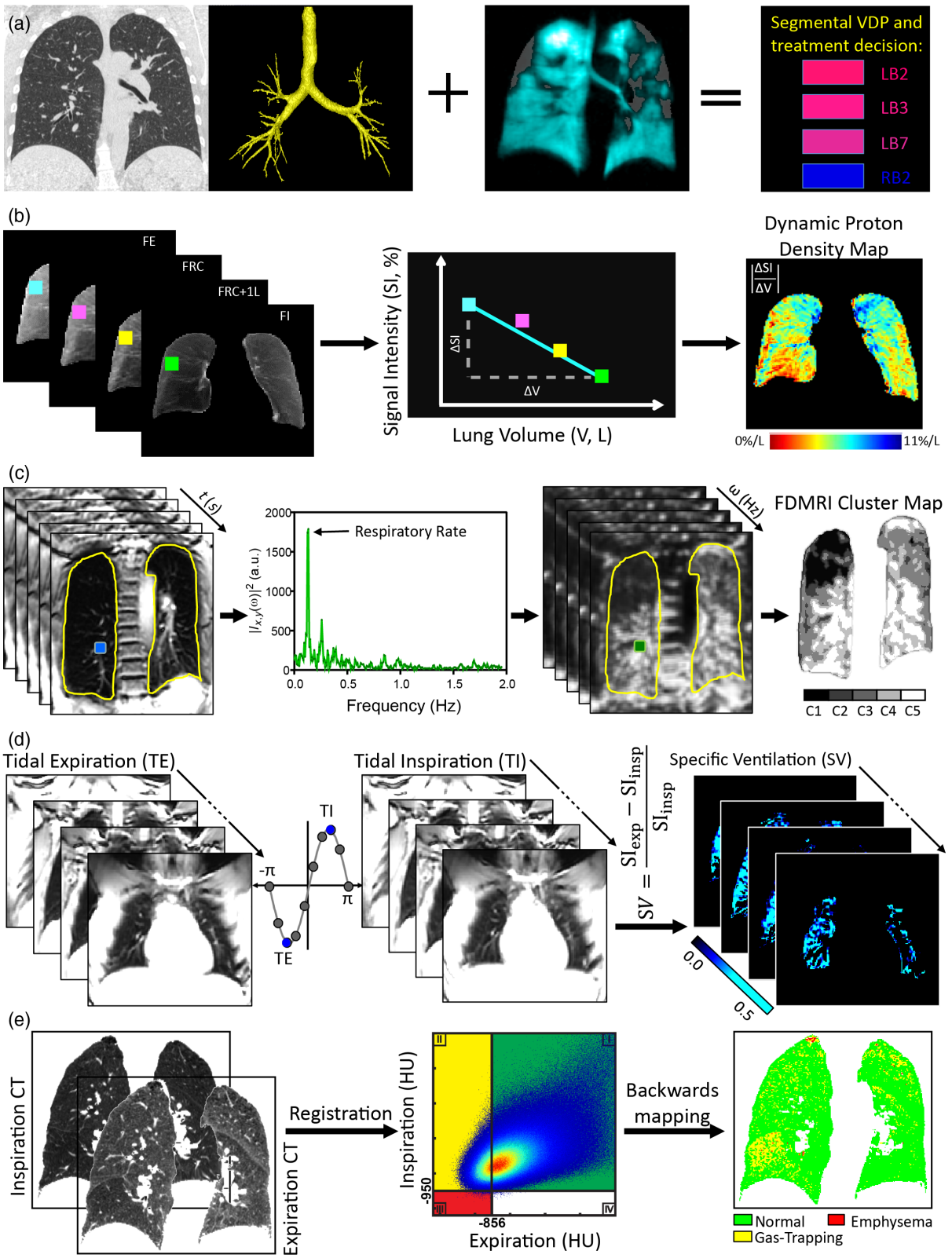

Fig. 3 Pulmonary imaging biomarker tools. (a) Whole lung, lobar, and segmental structure–function measurements using CT and noble gas MRI. (b) Dynamic proton density measurements using multivolume UTE MRI. (c) 2-D and (d) 3-D free-breathing lung structure–function measurements. (e) Inspiration–expiration CT parametric response mapping.

2.2 *Whole Lung and Regional Structure and Function Using Inhaled Gas MRI*

Inhaled gas MRI using ^{19}F[45] and hyperpolarized ^{3}He/^{129}Xe[12] provides a way to visualize lung airway/airspace microstructure as well as gas distribution/ventilation. The quantitative analysis of inhaled gas MRI structural–functional information depends on both thoracic cavity segmentation and structure–function image coregistration.[40] This framework provides both an interactive ^{1}H-^{3}He MRI lung segmentation method[40] and an automated ^{1}H-^{3}He MRI joint segmentation approach that utilize convex optimization techniques.[41] Whole lung ventilation abnormalities (^{3}He/^{129}Xe) may be quantified using a hierarchical K-means clustering method[40] to generate whole lung ventilation maps and ventilation defect percent (VDP),[40] the volume of ventilation abnormalities (from ^{3}He/^{129}Xe MRI) normalized to the volume of the thoracic cavity (from ^{1}H MRI). For regional VDP measurements, CT-^{1}H/^{3}He MRI joint deformable registration[42] and CT lobe masks identified using other commercial software including Pulmonary Workstation 2.0 (VIDA Diagnostic Inc., Corallville, Iowa) may be easily integrated within this GUI. Similar to whole lung measurements, lobar and segmental ^{3}He/^{129}Xe MRI VDP may be generated by normalizing ^{3}He/^{129}Xe ventilation defect volumes to CT lung lobar and segmental volumes.[46]

2.3 *Ultrashort Echo-Time* ^{1}H MRI*: Static and Dynamic Proton Density*

UTE MRI provides enhanced visualization of the lung parenchyma and is ideally suited for the evaluation of pediatric patients[44] but lung segmentation is also required as a first step. This framework provides a UTE MRI lung segmentation approach using high-dimensional features combining heterogeneous image signal intensities and coordinate space information.[47] These features were distinguished using a kernel K-means-based machine-learning approach.[48] The derived high-order feature clustering term was simplified through linearization and was entered into a continuous max-flow/min-cut segmentation formulation[49] that regularized the segmentation boundary smoothness. Fully automated lung segmentation was performed by registering a single atlas image and transforming the atlas lung mask to initialize the max-flow/min-cut segmentation model with high-order features. The output from the segmentation model was looped back and this step was iterated until convergence and the final segmentation was achieved. The segmented lung volumes can then be used for static and dynamic signal intensity measurements.[19,44]

2.4 *Free-Breathing* ^{1}H MRI *Fourier-Decomposition: Ventilation and Perfusion*

FDMRI provides a way to generate ventilation and perfusion maps using conventional ^{1}H MRI without exogenous contrast.[22] We developed an FDMRI image analysis pipeline by integrating free-breathing ^{1}H MRI lung series segmentation, registration, Fourier analysis as well as ventilation and perfusion quantification.[50] Free-breathing ^{1}H MRI series were simultaneously segmented using a coupled Potts model[49] by employing the inherent similarity of lung segmentation between adjacent slices. The segmented lung series were registered together using a coarse-to-fine deformable registration framework[42] that employed a modality-independent-neighborhood descriptor[51] and total variation of the displacement field for registration regularization. Pairwise registrations were implemented in parallel and the registered lung volumes were used for Fourier analysis; Fourier spectrum magnitudes at the respiratory and cardiac frequencies (determined using respiratory bellow data) were used to generate ventilation and perfusion maps.[21]

2.5 *Free-Breathing* ^{1}H MRI*: Specific Ventilation*

Conventional free-breathing ^{1}H MRI also provides a way to generate SV maps and values. Approximately 50 free-breathing ^{1}H MRI images acquired during two to three breathing cycles are sorted into 10 respiratory phase points ($-\pi \sim \pi$) and stacked into a single 3-D ^{1}H-MRI volume for each respiratory phase point.[52] The tidal expiration and inspiration 3-D ^{1}H-MRI volumes are coregistered using an optical flow-based registration approach,[53] and SV is calculated for each voxel using the registered inspiration and expiration image signal intensities (SI_{insp} and SI_{exp}) as follows:

$$SV = \frac{SI_{exp} - SI_{insp}}{SI_{insp}}. \quad (1)$$

2.6 *Multimodality Parametric Response Maps*

PRM of inspiration and expiration CT[54] has been used to classify lung image voxels as normal, emphysematous, or gas trapping due to small airways disease.[55] This tool provides automated PRM results using rigid and deformable registration tools[42] required for CT inspiration–expiration, MRI-to-CT, or MRI-to-MRI PRM maps.

2.7 *Radiomics*

Radiomics tools are provided to generate image features including mean, standard deviation, variance, gradient of image signal intensities, uniformity and size of object of interest, entropy/correlation, neighborhood connection, and other high-order features.[56,57] Optimal features can be classified using machine learning techniques and combined with high-throughput algorithms such as bound relaxation and convex optimization.[41,42,48] These tools provide enormous promise to better understand lung disease, build and improve clinical decision support systems.[58,59]

3 Results

Figure 4 shows CT airway-^{3}He MRI registration, multivolume UTE MRI dynamic proton density, 2-D FDMRI ventilation, and 3-D free-breathing ^{1}H MRI SV measurements of a representative asthma and COPD patient. This tool now provides a number of lung MRI and CT biomarkers, including: (1) whole lung, lobar, and segmental noble gas MRI ventilation volume, ventilation defect volume (VDV), VDP, (2) whole lung, lobar, and segmental noble gas apparent diffusion coefficient, (3) UTE MRI static and dynamic proton density, (4) conventional and free-breathing ^{1}H MRI ventilation and perfusion, (5) CT and MRI RPM measurements, and (6) radiomics biomarkers.

Using a Windows desktop (Windows 8.1, 32G RAM, Inter (R) i7-3770 CPU, and NVIDIA GTX TITAN BLACK GPU), the interactive segmentation method[40] required 15 min for each patient. For a diverse patient group ($n = 15$) with asthma, COPD, and cystic fibrosis, this method achieved DSC of 91% for ventilation regions, 44% for ventilation defect regions, and

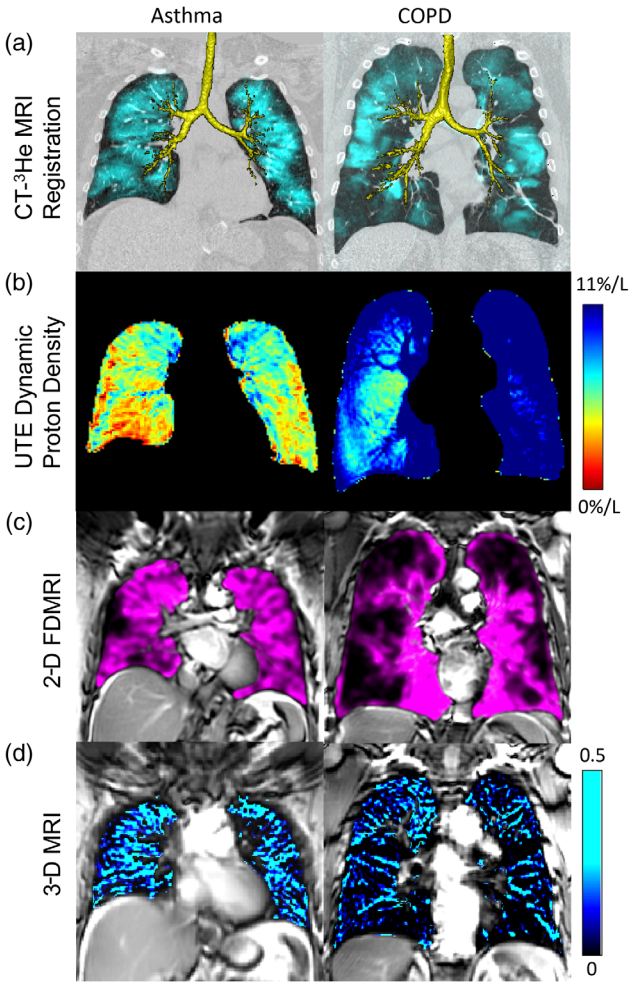

Fig. 4 Pulmonary MRI and CT biomarker outputs for representative asthma and COPD patient. (a) CT-^{3}He MRI registration (lung lobes and segments not shown). (b) UTE dynamic proton density maps. (c) FDMRI ventilation measurements. (d) 3-D free-breathing MRI-specific ventilation measurements.

strong correlations between algorithm and manual ventilation/ventilation defects volumes (all Pearson $r > 0.84$, $p < 0.001$). For repeated segmentation of ventilation defect volumes, intra- and interobserver coefficient of variation was 5% and 7%, respectively, and a smallest detectable difference of 0.11 L was achieved.[40] The automated ^{1}H-^{3}He MRI cosegmentation approach[41] yielded a DSC of 91%, surface distance error of 4.3 mm, and percentage volume error of 5.4% in 0.5 min with high intra- and interobserver reproducibility on a clinical dataset of 25 COPD patients at various disease stages. This approach[41] was later applied to 12 healthy and COPD patients and achieved a coefficient of variation of 4% for VDP measurements that were not significantly different ($p = 0.14$)[60] from a reference segmentation method. The fully automated whole lung, lobar, and segmental CT-^{3}He/^{129}Xe MRI structure–function measurement method[42] provided a CT-^{3}He MRI target registration error of 4.4 mm on a dataset of 35 asthma and COPD patients at different stages. This approach[42] required 10 min for each subject and the derived whole lung VDP measurements were not significantly different from a semiautomated method ($p = 0.37$). The semiautomated segmentation method[47] for statistic and dynamic UTE proton density measurements yielded a DSC of 93%, surface distance of 3 mm with a coefficient of variation <2% on 10 asthma patients. This interactive segmentation[47] method required 2 min to segment each 3-D image, and a fully automated UTE segmentation and quantification pipeline is under development. Anatomic ^{1}H MRI lung segmentation was required for FD and multivolume SV measurements. The 2-D free-breathing ^{1}H MRI segmentation-registration pipeline[50] achieved DSC of 96% and 97% for lung series segmentation and registration, respectively, and 4% coefficient of variation for FD-VDP measurements. This module[50] required 10 min for each subject and generated FD-VDP measurements that were strongly correlated with ^{3}He-VDP in 10 COPD patients. The 3-D ^{1}H MRI lung segmentation approach[43] yielded a DSC of 91%, surface distance of 4.0 mm, and absolute percent volume error of 6% in 0.2 min in a group of 20 asthma patients. This segmentation approach[43] was applied to 23 asthma and seven healthy subjects,[52] and yielded multivolume ^{1}H MRI SV measurements that were significantly correlated with ^{3}He-VDP ($r = 0.67$, $p < 0.0001$). CT was segmented with Pulmonary Workstation (VIDA Diagnostic Inc., Corallville, Iowa) and the segmented inspiration–expiration lung registration was performed using an affine and deformable registration approach that demonstrated landmark registration error of 0.75 mm.[61] For a group of 58 exsmokers,[55] inspiration–expiration CT PRM gas trapping ($r = 0.58$, $p < 0.001$) and emphysema ($r = 0.68$, $p < 0.001$) were generated in 2 min and were significantly correlated with reference ^{3}He-VDP measurements.

These individual algorithms were implemented by users at different experience levels and were comprehensively evaluated and tested on diverse patient dataset across a wide range of disease states. Therefore, we think these functional modules are robust and have the potential for broad research and clinical applications. In addition, the computational efficiency of the biomarker platform can be further improved with higher-end hardware and algorithm automation. As currently implemented, the interactive ^{1}H-^{3}He MRI structure–function measurement module[40] required manual identification of three to seven pairs of corresponding landmarks in center ^{1}H and ^{3}He MRI slices. Errors in ^{1}H MRI lung cavity segmentation and ^{3}He MRI ventilation clustering were manually corrected by adding or removing regions in respective images based on visual inspection. The automated ^{1}H-^{3}He MRI cosegmentation method[41] required user sampling of each lung and the background on a single coronal plane. The coronal slices were chosen when the segmentation was deemed challenging, e.g., protruding structures, weak separation between lung and the mediastinum/chest wall. The same seeding procedures were used for 3-D UTE,[47] 2-D free-breathing,[50] and 3-D single or multivolume ^{1}H MRI segmentation.[43] These are the biomarker modules that required user interaction while the others[42,46,50,55] are fully automated.

4 Discussion

The current and growing burden of chronic lung disease on patients and healthcare systems requires new tools and biomarkers to help develop new treatments, deeply phenotype patients, and optimize treatments and outcomes. To address this need, we developed a pulmonary MRI and CT biomarker pipeline as a first step toward our larger efforts to enable high-throughput pulmonary MRI and CT biomarkers for lung disease patient care.

While pulmonary MRI and CT biomarkers are being increasingly used, gaps remain in the translation of imaging research to clinical research workflows, due in part, to a lack of practical and point-of-care tools to generate imaging biomarkers. Our biomarker framework provides a GUI-based, user friendly way to rapidly generate lung MRI and CT biomarkers automatically or via minimal user interactions that do not require special expertise. These GUI-based push-button biomarker pipelines facilitate user interaction and visualization, require minimal workload, and provide high flexibility and reproducibility, suggesting the translational potential for high-throughput clinical workflows. We have installed the prototype software on a number of Windows tablets and have provided these to Centre for Heart Lung Innovation, St. Paul's Hospital (University of British Columbia, Vancouver, British Columbia, one site) last year. We also have units ready for testing at London Health Sciences Centre (London, Ontario, two sites) and St. Joseph's Health Care (McMaster University, Hamilton, Ontario, one site). Other ways of implementing this approach include integrating our algorithms as plug-ins into pre-existing frameworks (e.g., 3-D Slicer[62] and MITK[63]), which are well-tested and provide robust implementation of commonly used functionalities. While we certainly can (and will, in the near future) add our utilities as plug-ins to existing frameworks, we believe that this will not help advance the use of quantitative imaging among pulmonologists at the bedside, nor in clinic when and where physicians make treatment decisions. In other words, our overarching goal is to provide a tablet platform for generating straightforward measurements while the patient is still in clinic. Moreover, we want to emphasize that our GUI-based biomarker implementation was targeted for pulmonary applications and has application-specific requirements, e.g., multiview 3-D volume rendering as shown in Fig. 1, which were identified as critical by our local and remote clinicians and end users. Although some of the required functionality is provided by existing frameworks, these application-specific features were not supported nor are these frameworks used in respirology or radiology clinical workflows, which we believe has limited translation. Therefore, here we collaborated with Dr. Aaron Fenster's software development team with more than 15 years' experience and developed this point-of-care framework by integrating these application-specific functionality and image-processing algorithms. We also note that these individual algorithms integrated in the GUI were developed from scratch using C++ and/or CUDA, and only standard and basic libraries were used. Therefore, we think these algorithms are flexible and independent from the GUI, suggesting that data processing can happen offline with the capability of cross-platform, cross-applications. We note that currently these algorithms provide high computational performance, flexibility, and they are platform-independent. While these algorithms are currently embedded in a GUI-oriented software framework on a dedicated Windows desktop/tablet that facilitates user interaction and visualization, we also previously implemented these via efficient command lines that are aimed to enable the analysis of large datasets.

It is our vision was to develop a free, open-source, and multi-platform pulmonary imaging biomarker framework and bring this tool to the clinic, for point-of-care use, based on the requirements of our clinical collaborators. We think that a tablet GUI will help accelerate the translation of imaging biomarkers to clinical use more efficiently than cloud-based or workstation-based algorithms, because clinicians use measurements in real-time while seeing the patient. For this reason, we optimized the compatibility of our software framework within Windows-based PC tablets typically used in the clinic environment. However, in recognition of the complex clinical environment, our biomarker framework must be optimized and this will be ensured in future by a commitment to continuous development, testing, and lifecycle maintenance. The development of the software application originates from our group and contributions in all aspects are welcome to improve the tool. For example, the developer team will perform system design/lifecycle maintenance and functional testing, provide source code and test data, tutorial, documentation, and training to end users; potential developers and those who are interested in this tool can apply and approved applicants can participate in the development; end users can report bugs and provide requirements and feedback of using the tool to the developer team. We also note that pulmonary imaging biomarkers are emerging rapidly, and the tool we developed represents a flexible biomarker tool that is expandable. New biomarkers, once validated within the pulmonary imaging community, may be easily integrated within this tool and distributed to end users. For this purpose, we reserved interfaces with specifications so users can add other functionality into the framework.

Our current efforts are focused on development and validation of new data analysis algorithms and biomarker modules as well as robust software integration. We also note that end-user feedback is a main driver for the development of the biomarker framework and through continuous interaction with our clinical collaborators, we have together determined a number of components that are urgently needed. These components include: (1) 3-D visualization of the spatial relationship between MRI ventilation defects and airway tree, and navigation of surgical tools, (2) disease phenotyping through feature engineering of clinical, histological, biological, and imaging measurements using deep learning, and (3) portable tablet implementation of the biomarker tools for point-of-care clinical applications. These critical requirements need substantial efforts for the completion of the biomarker framework development and represent our ongoing work with high priorities. It is also well recognized that advancing lung MRI and CT toward broader clinical applications requires global collaboration and validation of clinically relevant biomarkers in multicenter research and clinical trials.[33] In this regard, standardization of image analysis tools is critically required to increase the power of cross-center comparison and to facilitate a deeper understanding of lung MRI and CT biomarkers.[33] Motivated by previous studies[64] that provided a lung CT database to the pulmonary imaging community, we set up our long-term work plan to provide a potentially standardized and universally available biomarker tool to facilitate high-throughput research and point-of-care clinical applications of pulmonary MRI and CT. In line with our long-term work plan, we are making every effort to share the source code, dependent libraries, and compiled binary executables on public repositories. Release of a stable version of the software is crucial for the pulmonary imaging research community, and it is well recognized that software development process requires intensive and extensive efforts from all aspects. We now have published the main components in our biomarker framework on our lab website (http://www.imaging.robarts.ca/parraga/technology_codes.html) as well as on Github (available in Github repository: https://github.com/fumguo/Pulmonary-MRI-and-CT-biomarker-framework). These components include

the software GUI and dependent libraries, a number of image segmentation and registration algorithms, and biomarker quantification methods. We also provided test demos (mainly MATLAB scripts for simplicity) for readers who are interested in specific biomarker modules. We note that this is not a complete version of the source code because: (1) the licensing regulations of the 3-D visualizer (contact us for licensing), (2) confidentiality of unpublished work, and (3) the ongoing work on the prioritized components recently identified by our clinical collaborators. In this regard, we are working in collaboration with a software development team (more than 15 years experience) and an image processing and biomarker quantification group (more than 10 years experience) to expedite the development of the biomarker tool. We aim to finish the unpublished work as soon as possible and release a complete version of the source code for the biomarker framework in 1 year.

Our approach also integrates high-performance computational modeling and optimization algorithms as well as machine learning techniques to extract hidden lung disease information from high-dimensional pulmonary MRI and CT. For example, the integrated computational optimization algorithms may be readily employed to develop high-performance image denoising, MRI-MRI and MRI-CT image fusion, lung registration for atlas construction, fast and high-resolution image acquisition with compressed sensing and parallel imaging. We also realized that using imaging data exclusively may not warrant a deep understanding of lung disease, and the combination of information from multiple sources may provide added value. In the era of "big data," the invaluable complementary physiological, histological, biological, and genetic information may be combined with imaging findings to generate a clearer picture of chronic lung disease through data mining and perhaps facilitate the development of "precision medicine." The utilization of complex information from multiple sources involves dimension reduction, advanced computation, and optimization methods as well as machine learning techniques. It is in this context that we think a lung imaging biomarker tool may provide added value to advance not only lung disease but also other disease studies.

5 Conclusions

We developed a user-friendly pulmonary imaging biomarker analysis tool that provides validated and emerging pulmonary MRI and CT biomarkers, including lung ventilation, perfusion, parenchyma morphology, texture, and gas trapping. Our biomarker tool and framework integrates a series of validated high-performance image processing and analysis algorithms, and automatically generates these biomarker measurements with minimal user interactions, high-computational efficiency, and reproducibility. We think that this approach provides the translational potential for high-throughput research and clinical studies and point-of-care decision making.

Disclosures

No conflicts of interest, financial or otherwise, are declared by the authors.

Acknowledgments

Dr. Parraga gratefully acknowledges funding from a Canadian Institutes of Health Research Team Grant CIF #97687 (Thoracic Imaging Network of Canada). Guo is currently supported by a postdoctoral fellowship from the Natural Sciences and Engineering Research Council of Canada (NSERC). Capaldi was supported by an NSERC doctoral scholarship.

References

1. H. O. Coxson et al., "Using pulmonary imaging to move chronic obstructive pulmonary disease beyond FEV1," *Am. J. Respir. Crit. Care Med.* **190**(2), 135–144 (2014).
2. National Emphysema Treatment Trial Research Group, "Rationale and design of the National Emphysema Treatment Trial: a prospective randomized trial of lung volume reduction surgery," *Chest J.* **116**(6), 1750–1761 (1999).
3. N. N. Jarjour et al., "Severe asthma: lessons learned from the national heart, lung, and blood institute severe asthma research program," *Am. J. Respir. Crit. Care Med.* **185**(4), 356–362 (2012).
4. D. E. Bild et al., "Multi-ethnic study of atherosclerosis: objectives and design," *Am. J. Epidemiol.* **156**(9), 871–881 (2002).
5. E. A. Regan et al., "Genetic epidemiology of COPD (COPDGene) study design," *J. Chronic Obstruct. Pulm. Dis.* **7**(1), 32–43 (2011).
6. J. Bourbeau et al., "Canadian cohort obstructive lung disease (CanCOLD): fulfilling the need for longitudinal observational studies in COPD," *J. Chronic Obstruct. Pulm. Dis.* **11**(2), 125–132 (2014).
7. J. Vestbo et al., "Evaluation of COPD longitudinally to identify predictive surrogate end-points (ECLIPSE)," *Eur. Respir. J.* **31**(4), 869–873 (2008).
8. D. Couper et al., "Design of the subpopulations and intermediate outcomes in COPD study (SPIROMICS)," *Thorax* **69**, 491–494 (2013).
9. D. A. Lynch et al., "CT-definable subtypes of chronic obstructive pulmonary disease: a statement of the Fleischner society," *Radiology* **277**(1), 192–205 (2015).
10. P. G. Woodruff et al., "Clinical significance of symptoms in smokers with preserved pulmonary function," *N. Engl. J. Med.* **374**(19), 1811–1821 (2016).
11. J. P. Sieren et al., "SPIROMICS protocol for multicenter quantitative computed tomography to phenotype the lungs," *Am. J. Respir. Crit. Care Med.* **194**(7), 794–806 (2016).
12. M. Albert et al., "Biological magnetic resonance imaging using laser-polarized ^{129}Xe," *Nature* **370**(6486), 199–201 (1994).
13. D. A. Yablonskiy et al., "Quantification of lung microstructure with hyperpolarized ^{3}He diffusion MRI," *J. Appl. Physiol.* **107**(4), 1258–1265 (2009).
14. B. T. Saam et al., "MR imaging of diffusion of ^{3}He gas in healthy and diseased lungs," *Magn. Reson. Med.* **44**(2), 174–179 (2000).
15. J. Vogel-Claussen et al., "Quantification of pulmonary inflammation after segmental allergen challenge using turbo-inversion recovery-magnitude magnetic resonance imaging," *Am. J. Respir. Crit. Care Med.* **189**(6), 650–657 (2014).
16. R. R. Edelman et al., "Noninvasive assessment of regional ventilation in the human lung using oxygen-enhanced magnetic resonance imaging," *Nat. Med.* **2**(11), 1236–1239 (1996).
17. L. L. Walkup et al., "Quantitative magnetic resonance imaging of bronchopulmonary dysplasia in the neonatal intensive care unit environment," *Am. J. Respir. Crit. Care Med.* **192**(10), 1215–1222 (2015).
18. A. R. Morgan et al., "Feasibility assessment of using oxygen-enhanced magnetic resonance imaging for evaluating the effect of pharmacological treatment in COPD," *Eur. J. Radiol.* **83**(11), 2093–2101 (2014).
19. W. Ma et al., "Ultra-short echo-time pulmonary MRI: evaluation and reproducibility in COPD subjects with and without bronchiectasis," *J. Magn. Reson. Imaging* **41**(5), 1465–1474 (2015).
20. C. Bergin, J. Pauly, and A. Macovski, "Lung parenchyma: projection reconstruction MR imaging," *Radiology* **179**(3), 777–781 (1991).
21. D. P. Capaldi et al., "Free-breathing pulmonary ^{1}H and hyperpolarized ^{3}He MRI: comparison in COPD and bronchiectasis," *Acad. Radiol.* **22**(3), 320–329 (2015).
22. G. Bauman et al., "Non-contrast-enhanced perfusion and ventilation assessment of the human lung by means of Fourier decomposition in proton MRI," *Magn. Reson. Med.* **62**(3), 656–664 (2009).
23. M. Kirby et al., "Chronic obstructive pulmonary disease: longitudinal hyperpolarized ^{3}He MR imaging," *Radiology* **256**(1), 280–289 (2010).
24. S. Fain et al., "Severe asthma research program-phenotyping and quantification of severe asthma," *Imaging Decis. MRI* **13**(1), 24–27 (2009).

25. M. Kirby et al., "MRI ventilation abnormalities predict quality-of-life and lung function changes in mild-to-moderate COPD: longitudinal TINCan study," *Thorax* **72**, 475–477 (2017).
26. H.-U. Kauczor et al., "Normal and abnormal pulmonary ventilation: visualization at hyperpolarized He-3 MR imaging," *Radiology* **201**(2), 564–568 (1996).
27. G. Parraga et al., "Hyperpolarized ^{3}He magnetic resonance imaging of ventilation defects in healthy elderly volunteers: initial findings at 3.0 Tesla," *Acad. Radiol.* **15**(6), 776–785 (2008).
28. S. Samee et al., "Imaging the lungs in asthmatic patients by using hyperpolarized helium-3 magnetic resonance: assessment of response to methacholine and exercise challenge," *J. Allergy Clin. Immunol.* **111**(6), 1205–1211 (2003).
29. M. Kirby et al., "Chronic obstructive pulmonary disease: quantification of bronchodilator effects by using hyperpolarized He MR imaging," *Radiology* **261**(1), 283–292 (2011).
30. R. P. Thomen et al., "Regional ventilation changes in severe asthma after bronchial thermoplasty with ^{3}He MR imaging and CT," *Radiology* **274**(1), 250–259 (2014).
31. S. Svenningsen et al., "Is ventilation heterogeneity related to asthma control?" *Eur. Respir. J.* **48**(2), 370–379 (2016).
32. D. A. Hoover et al., "Functional lung avoidance for individualized radiotherapy (FLAIR): study protocol for a randomized, double-blind clinical trial," *BMC Cancer* **14**(1), 934 (2014).
33. D. P. I Capaldi, R. L. Eddy, and G. Parraga, "Pulmonary MRI in clinical trials," in *Medical Radiology*, Springer, Berlin, Heidelberg (2018).
34. E. A. Hoffman et al., "Pulmonary CT and MRI phenotypes that help explain chronic pulmonary obstruction disease pathophysiology and outcomes," *J. Magn. Reson. Imaging* **43**(3), 544–557 (2016).
35. A. Fenster, S. Dunne, and J. T. Larsen, "Three-dimensional imaging system," U. S. Patent No. 5,842,473 (1998).
36. VTK, "The visualization Toolkit: an object-oriented approach to 3D graphics," https://www.vtk.org (4 May 2018).
37. GDCM, "Grassroots DICOM library," http://gdcm.sourceforge.net/ (4 May 2018).
38. A. Fenster, D. B. Downey, and H. N. Cardinal, "Three-dimensional ultrasound imaging," *Phys. Med. Biol.* **46**(5), R67 (2001).
39. D. Cool et al., "Design and evaluation of a 3-D transrectal ultrasound prostate biopsy system," *Med. Phys.* **35**(10), 4695–4707 (2008).
40. M. Kirby et al., "Hyperpolarized ^{3}He magnetic resonance functional imaging semiautomated segmentation," *Acad. Radiol.* **19**(2), 141–152 (2012).
41. F. Guo et al., "Globally optimal co-segmentation of three-dimensional pulmonary ^{1}H and hyperpolarized ^{3}He MRI with spatial consistence prior," *Med. Image Anal.* **23**(1), 43–55 (2015).
42. F. Guo et al., "Thoracic CT-MRI coregistration for regional pulmonary structure–function measurements of obstructive lung disease," *Med. Phys.* **44**(5), 1718–1733 (2017).
43. F. Guo et al., "Anatomical pulmonary magnetic resonance imaging segmentation for regional structure-function measurements of asthma," *Med. Phys.* **43**(6), 2911–2926 (2016).
44. K. Sheikh et al., "Ultrashort echo time MRI biomarkers of asthma," *J. Magn. Reson. Imaging* **45**(4), 1204–1215 (2017).
45. B. J. Soher et al., "Lung imaging in humans at 3T using perfluorinated gases as MR contrast agents," in *Proc. of Int. Society for Magnetic Resonance*, Vol. 3389 (2010).
46. F. Guo et al., "Automated pulmonary lobar ventilation measurements using volume-matched thoracic CT and MRI," *Proc. SPIE* **9417**, 941717 (2015).
47. F. Guo et al., "Ultra-short echo-time MRI lung segmentation using high-dimensional features and continuous max-flow," in *Proc. of Int. Society for Magnetic Resonance*, Vol. 4024 (2017).
48. M. Tang et al., "Secrets of GrabCut and kernel K-means," in *Proc. IEEE Int. Conf. on Computer Vision*, pp. 1555–1563 (2015).
49. J. Yuan et al., "A continuous max-flow approach to Potts model," in *Computer Vision–ECCV 2010*, pp. 379–392 (2010).
50. F. Guo et al., "Registration pipeline for pulmonary free-breathing ^{1}H MRI ventilation measurements," *Proc. SPIE* **10137**, 101370A (2017).
51. M. P. Heinrich et al., "MIND: modality independent neighbourhood descriptor for multi-modal deformable registration," *Med. Image Anal.* **16**(7), 1423–1435 (2012).
52. D. P. Capaldi et al., "Free-breathing pulmonary MR imaging to quantify regional ventilation," *Radiology* **287**, 693–704 (2018).
53. B. D. Lucas and T. Kanade, "An iterative image registration technique with an application to stereo vision" in *Proc. of the 7th Int. Joint Conf. on Artificial Intelligence (IJCAI 1981)*, pp. 674–679, Morgan Kaufmann Publishers Inc., San Francisco, California (1981).
54. C. J. Galbán et al., "The parametric response map is an imaging biomarker for early cancer treatment outcome," *Nat. Med.* **15**(5), 572–576 (2009).
55. D. P. Capaldi et al., "Pulmonary imaging biomarkers of gas trapping and emphysema in COPD: ^{3}He MR imaging and CT parametric response maps," *Radiology* **279**(2), 597–608 (2016).
56. N. Zha et al., "Second-order texture measurements of ^{3}He ventilation MRI: proof-of-concept evaluation of asthma bronchodilator response," *Acad. Radiol.* **23**(2), 176–185 (2016).
57. S. A. Mattonen et al., "Early prediction of tumor recurrence based on CT texture changes after stereotactic ablative radiotherapy (SABR) for lung cancer," *Med. Phys.* **41**(3), 033502 (2014).
58. P. Lambin et al., "Radiomics: extracting more information from medical images using advanced feature analysis," *Eur. J. Cancer* **48**(4), 441–446 (2012).
59. R. J. Gillies, P. E. Kinahan, and H. Hricak, "Radiomics: images are more than pictures, they are data," *Radiology* **278**(2), 563–577 (2015).
60. F. Guo et al., "A segmentation pipeline for measuring pulmonary ventilation suitable for clinical workflows and decision-making," in *Proc. of Int. Society for Magnetic Resonance*, Vol. 1609 (2016).
61. K. Murphy et al., "Evaluation of registration methods on thoracic CT: the EMPIRE10 challenge," *IEEE Trans. Med. Imaging* **30**(11), 1901–1920 (2011).
62. 3D slicer, "3D slicer software," https://www.slicer.org/ (4 May 2018).
63. MITK, "The medical imaging interaction Toolkit (MITK)," http://mitk.org/wiki/MITK (4 May 2018).
64. S. G. Armato, III et al., "Lung image database consortium: developing a resource for the medical imaging research community," *Radiology* **232**(3), 739–748 (2004).

Fumin Guo is a NSERC-funded postdoctoral fellow at Sunnybrook Research Institute, University of Toronto, Toronto, Canada. He received his BEng degree in bioinformatics from Huazhong University of Science and Technology (HUST), Wuhan, China, in 2009, his MESc degree in biomedical engineering from HUST in 2012, and his PhD in biomedical engineering from the Graduate Program, Robarts Research Institute, the University of Western Ontario, London, Canada, in 2017. Since 2014, he has authored 22 peer-reviewed manuscripts and his current research interests include pulmonary and cardiovascular imaging, medical image processing, optimization, computer vision, and machine learning.

Dante Capaldi is currently a NSERC-funded PhD student at the University of Western Ontario, London, Canada. He received his BSc (Hons) degree from the University of Windsor, Windsor, Canada, in 2013. Since 2013, he has authored 17 peer-reviewed manuscripts and his current interests include image processing and image-guided radiation therapy.

Miranda Kirby is currently a CIHR Banting postdoctoral fellow at the University of British Columbia, Vancouver, Canada. She received her BSc (Hons) and PhD degrees from the University of Western Ontario, London, Canada, in 2013. Since 2010, she has authored 50 peer-reviewed manuscripts and her current interests include the development and validation of CT airway biomarkers of COPD.

Khadija Sheikh is currently a clinical physics resident at Johns Hopkins University School of Medicine, Baltimore, Maryland, USA. She received her BSc (Hons) degree from the University of Windsor, Windsor, Canada, and PhD from the University of Western Ontario, London, Canada, in 2016. Since 2012, she has authored 17 peer-reviewed manuscripts and her current interests include radiation therapy and image-guided radiation therapy.

Sarah Svenningsen is currently a CIHR-funded postdoctoral fellow at McMaster University, Hamilton, Canada. She received her BSc (Hons) and PhD degrees from the University of Western Ontario, London, Canada, in 2015. Since 2011, she has authored

30 peer-reviewed manuscripts and her current interests include pulmonary MRI and inflammometry of severe asthma.

David G. McCormack is currently a professor of medicine and chair-chief respirology at the University of Western Ontario and London Health Sciences Centre, in London, Canada. He completed his MD training at Queens University and Respirology training at the University of Western Ontario. Since 2007, he has coauthored more than 100 manuscripts in collaboration with Dr. Parraga's team and his current interests include lung imaging biomarkers to optimize patient therapy decisions and outcomes.

Aaron Fenster is a professor at the University of Western Ontario, London, Canada. He received his BSc, MA, and PhD degrees from the University of Toronto, Toronto, Canada, in 1971, 1973, and 1976, respectively. He was the founder and director of the Imaging Research Laboratories of the Robarts Research Institute, where he is still a Robarts Scientist. He has authored 336 peer-reviewed publications 36 book chapters and six books. His current research is focused on image-guided interventions using 3-D ultrasound imaging fused with images from other modalities. He is a fellow of SPIE, IEEE, CCPM, AHS, and COMP.

Grace Parraga is a faculty scholar and professor at the University of Western Ontario as well as Scientist, Robarts Research Institute, in London, Canada. She received her BSc (Hons) and MSc degrees from the University of Western Ontario, London, Canada, and her PhD at the University of Washington, Seattle, Washington, USA, in 1990. Along with her lab team, she has authored more than 200 peer-reviewed manuscripts, book chapters, and conference proceedings in the past 13 years. Her current research interests include lung imaging biomarker development, image-guided pulmonary applications, and CT-MRI image processing.